Int. J. Heat Mass Transfer. Vol. 25, No. 11, pp. 1651–1660, 1982
Printed in Great Britain

0017–9310/82/111651–10 $03.00/0

GENERALIZED LAMINAR HEAT TRANSFER FROM THE SURFACE OF A ROTATING DISK

S. E. TADROS
E. I. Du Pont de Nemours and Company, Experimental Station Laboratory, Wilmington, DE 19898, U.S.A.

and

F. F. ERIAN
Shell Development Company, Westhollow Research Center, P.O. Box 1380, Houston, TX 77001, U.S.A.

(*Received* 5 *October* 1981 *and in final form* 12 *March* 1982)

Abstract—The energy equation for the laminar incompressible flow induced by a large spinning disk is solved numerically for the 3-dim. temperature field generated by a diametrical, sector-shaped heat source located at the disk surface which is otherwise adiabatic. The heating is assumed to be sufficiently mild so as not to disturb the velocity field. Consequently, natural convection effects, as well as viscous dissipation heating, are neglected. The simple overrelaxation technique may be applied to obtain solutions for any specified radial and/or tangential distributions of surface temperature or heat flux. Results obtained for various Prandtl numbers and source angles indicate the existence of a conduction dominated region at low Reynolds numbers and a convection dominated region at high Reynolds numbers. Correlation between the local surface heat flux and the tangential wall shear stress is also given.

NOMENCLATURE

A, constant;
B, constant;
C, C_{I}, C_{II}, C_{IV}, C_{V}, constants;
c_p, specific heat at constant pressure;
D, constant;
d, fluid density;
F, dimensionless radial velocity;
f_ϕ, tangential friction factor;
G, dimensionless tangential velocity;
$\bar{G}$, dimensionless relative tangential velocity;
Gr, Grashof number;
H, dimensionless axial velocity;
h, $\bar{h}$, local and average heat transfer coefficients, respectively;
k, fluid thermal conductivity;
m, constant;
Nu, $\overline{Nu}$, local and average Nusselt numbers, respectively;
Pr, Prandtl number;
Q, dimensionless axial temperature gradient at the wall;
q, heat flux per unit area;
Re, Reynolds number, $\omega r^2/\nu$;
r, radial coordinate;
r_s, source outer radius;
T, local temperature;
T_0, characteristic temperature scale of the heat source;
T_∞, ambient temperature;
u, radial velocity;
v, tangential velocity;
w, axial velocity;
z, axial coordinate.

Greek symbols

α, thermal diffusivity;
δ, momentum boundary layer thickness;
δ_{th}, thermal boundary layer thickness;
Δ, represents a small change;
η, dimensionless axial coordinate, $z(\omega/\nu)^{1/2}$;
η', dimensionless axial coordinate, $z/(r_s\psi_s)$;
θ, dimensionless temperature;
μ, absolute viscosity;
ν, kinematic viscosity;
ρ, dimensionless radial coordinate, $r(\omega/\nu)^{1/2}$;
ρ', dimensionless radial coordinate, r/r_s;
ρ_s, dimensionless source outer radius;
ϕ, tangential coordinate;
ϕ_s, source sector angle;
ϕ_{sl}, source leading edge angle;
ϕ_{st}, source trailing edge angle;
ψ, dimensionless tangential coordinate, ϕ/π;
ψ', dimensionless tangential coordinate, ϕ/ϕ_s;
ψ_s, dimensionless source sector angle;
ψ_{sl}, dimensionless source leading edge angle;
ψ_{st}, dimensionless source trailing edge angle;
$\tau_{w\phi}$, tangential wall shear stress;
ω, disk angular velocity.

INTRODUCTION

HEAT transfer from a rotating body is of major importance in the analysis and design of turbomachinery, especially when high temperature fluids are present. The rotating disk offers a simplified model

with which more complex rotating components can be examined. Due to the simple geometrical configuration, analysis is considerably less involved than if the actual components were considered.

Flow and heat transfer characteristics in the 3-dim. boundary layer over a rotating disk have been studied extensively. In the present work, a method is presented to predict the heat transfer characteristics for a generalized heat source at the disk surface.

The structure of the laminar flow field induced by the rotation of a large disk in an infinite incompressible fluid has been first established by von Karman [1]. Later it was improved numerically by Cochran [2]. This structure has been experimentally verified by Cham and Head [3], Erian and Tong [4], and others.

Heat transfer from a rotating disk under laminar flow conditions has been studied extensively for an isothermal disk surface. Wagner [5] first established the heat transfer from an isothermal disk into air ($Pr = 0.72$) as $Nu = 0.335\,Re^{0.5}$. Millsaps and Pohlhausen [6], using different methods, found that $Nu = C\,Re^{0.5}$ for $1 < Pr < 10$, where C increases with Prandtl number. Sparrow and Gregg [7] further examined the effect of Prandtl number on heat transfer from an isothermal disk, and found that $Nu = C\,Re^{0.5}$ is valid for $0.01 < Pr < 10$, where the constant also increases with Prandtl number. Asymptotic relations were also found between C and Pr at very high and very low Prandtl numbers.

Hartnett [8] solved the heat transfer problem from a rotating disk with a power law radial temperature distribution, $(T - T_\infty) = Br^m$, at $Pr = 0.72$ and found that $Nu = C\,Re^{0.5}$ with the constant becoming larger with increasing m. Davies [9] proposed an approximate method to predict heat transfer from a rotating disk with arbitrary radial temperature distribution by applying the method of sources, i.e. the disk surface is regarded as an assembly of concentric circular heat sources forming the desired surface temperature distribution. An integral equation was developed to predict the heat transfer coefficient at the disk surface but was valid only at large Prandtl numbers when the thermal boundary layer was deeply embedded in the momentum boundary layer. Recently, Jeng, DeWitt and Lee [10] developed a unique analytical method to obtain the temperature field and the rate of heat transfer from an axisymmetric body in a forced flow field. The method was applied to a finite rotating disk with or without a free stream velocity and the results agreed well with the calculations of Chao and Grief [11] for the case of an isothermal disk. The method can also be used for a disk with an axisymmetric step change in surface temperature. Radial conduction was neglected in all these analytical solutions.

Experimentally, Kreith, Taylor and Chong [12] have fully investigated the heat transfer from an isothermal disk and have found that $Nu = 0.345\,Re^{0.5}$ for $Pr = 0.72$ under laminar conditions. Popiel and Boguslawski [13] have determined the combined effect of free and forced convection and have found $Nu = 0.33\,(Gr + Re^2)^{0.25}$ on an isothermal disk at $Pr = 0.71$. Many other experimental works are available.

Most of the heat transfer work previously accomplished on the rotating disk is for an isothermal surface. In most practical applications (a turbine wheel, for example) temperature fields are axisymmetric but depend on the radial direction. Recently, Oehlbeck and Erian [14] solved the axisymmetric line source problem.

The present work accommodates any radial and tangential distributions of temperature or heat flux at the disk surface which are symmetric about a disk diameter, and, shows the effects of Prandtl number, Reynolds number and conduction on surface heat transfer coefficients from sources in the form of sectors of varying angles. In addition to its usefulness as a generalized 3-dim. problem, wherein heat transfer coefficients can be obtained for localized heat sources of arbitrary geometry (an image source about a disk diameter must exist), direct correlation between the local heat transfer coefficient at the source and the wall shear stress is also derived.

ANALYSIS

The equations of motion for the flow due to a rotating disk have been solved exactly by von Karman [1] and the solution improved by Cochran [2]. Due to their consideration of an infinite disk rotating in an infinite fluid, similarity functions of the velocity, dependent on a single similarity variable, were obtained. These are defined as $F(\eta) = u/\omega r$, $G(\eta) = v/\omega r$, and $H(\eta) = w/(v\omega)^{1/2}$ where η is the dimensionless axial distance from the disk surface.

The introduction of a heat source at the disk surface will generate a temperature field $T(r, \phi, z)$ in its vicinity due to convection and conduction. If one ignores natural convection effects, significant errors will admittedly be introduced at high relative source temperatures and at very low Reynolds numbers, i.e. near the disk center. However, in most practical cases, forced convection is far more significant than free convection. Therefore, we shall ignore natural convection effects in this work which results in decoupling of the momentum and energy equations. As a consequence, the velocity functions, F, G and H, remain unchanged by the introduction of heat sources at the disk surface.

Having established the flow field, we now consider the energy equation in cylindrical coordinates which rotate with the disk for steady, incompressible laminar flow with constant fluid properties and neglecting viscous dissipation. The equation for the temperature is given by

$$dc_p\left\{u\frac{\partial T}{\partial r} + \frac{\bar{v}}{r}\frac{\partial T}{\partial \phi} + w\frac{\partial T}{\partial z}\right\} = k\left\{\frac{\partial^2 T}{\partial r^2} + \frac{1}{r}\frac{\partial T}{\partial r} + \frac{1}{r^2}\frac{\partial^2 T}{\partial \phi^2} + \frac{\partial^2 T}{\partial z^2}\right\} \quad (1)$$

where

$$\bar{v} = v - \omega r$$

and

$$\bar{v}/\omega r = G(\eta) - 1 = \bar{G}(\eta).$$

In this work the disk surface is assumed adiabatic except for a sector-shaped heat source diametrically located on the surface as shown in Fig. 1. Therefore, the source period is π. In the radial direction the temperature gradient at the disk center must vanish due to symmetry, and, at large r, the temperature should reach ambient values especially for a finite source length r_s. The periodicity of the geometry requires that the temperature field be periodic in the tangential direction. Also, the temperature at the disk center must be unique. At the heat source, either the surface temperature or the surface heat flux must be specified. Furthermore, the temperature is assumed to reach ambient conditions far above the disk.

Based on the above description, the boundary conditions become

$$\frac{\partial}{\partial r} T(0, \phi, z) = 0 \quad \text{due to radial symmetry,} \tag{2a}$$

$$T(\infty, \phi, z) = T_\infty, \tag{2b}$$

$$\left.\begin{aligned} T(r, \phi, z) &= T(r, \{\phi + \pi\}, z) \\ \frac{\partial}{\partial \phi} T(r, \phi, z) &= \frac{\partial}{\partial \phi} T(r, \{\phi + \pi\}, z) \end{aligned}\right\} \quad \text{due to field periodicity,} \tag{3a, 3b}$$

$$\left.\begin{aligned} \frac{\partial}{\partial z} T(r, \phi, 0) &= 0 \quad \text{when } \phi < \phi_{st} \text{ and } \phi > \phi_{sl} \text{ for all } r, \\ &= 0 \quad \text{when } r > r_s \text{ for all } \phi. \end{aligned}\right\} \tag{4a}$$

$$\frac{\partial}{\partial z} T(r, \phi, 0) \quad \text{specified function of } r \text{ and } \phi \text{ when } r \leqslant r_s, \text{ or} \tag{4a'}$$

$$T(r, \phi, 0) \quad \text{specified function of } r \text{ and } \phi \text{ when } r \leqslant r_s. \tag{4a''}$$

$$T(r, \phi, \infty) = T_\infty. \tag{4b}$$

The above boundary conditions are suitable for diametrical sources of any sector angle $\phi_s = \phi_{sl} - \phi_{st}$.

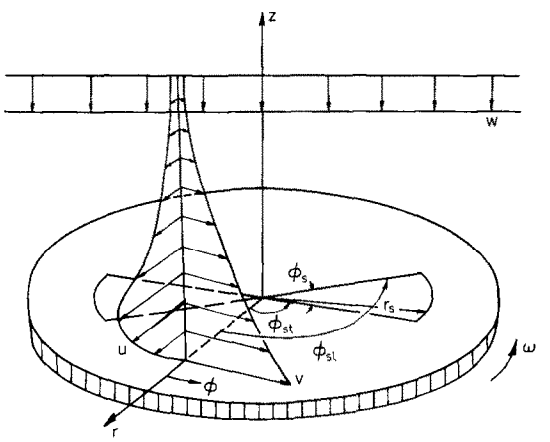

FIG. 1. Flow and source geometry.

Due to the periodicity of the problem, the solutions for more than one diametrical heat source may be obtained for source periods equaling even fractions of 2π, i.e. for sources located at $2\pi/n$, where $n = 2, 4, 6, \ldots$.

The energy equation may be nondimensionalized using appropriate characteristic lengths, velocity and temperature scales. In both the radial and axial directions the distance $(\nu/\omega)^{1/2}$ characteristic of the momentum boundary layer thickness, is a suitable scale, while in the azimuthal direction, the source period is appropriate. For the velocity and temperature, ωr and $(T_0 - T_\infty)$ are used. In this work T_0 is the maximum temperature of the source. Therefore, the following variables, in addition to the known velocity functions F, $\bar{G}$ and H, are introduced:

$$\rho = r(\omega/\nu)^{1/2}, \quad \rho_s = r_s(\omega/\nu)^{1/2}, \quad \eta = z(\omega/\nu)^{1/2},$$

$$\psi = \phi/\pi, \quad \theta = (T - T_\infty)/(T_0 - T_\infty), \quad Pr = \frac{\nu}{\alpha} = \frac{\mu c_p}{k}.$$

Substituting the above variables in equation (1) we obtain the dimensionless energy equation for $\theta = \theta(\rho, \psi, \eta)$

$$\frac{\partial^2\theta}{\partial\rho^2} + \frac{1}{\rho^2\pi^2}\frac{\partial^2\theta}{\partial\psi^2} + \frac{\partial^2\theta}{\partial\eta^2} + \frac{1}{\rho}(1 - \rho^2 PrF) \times \frac{\partial\theta}{\partial\rho} - \frac{Pr}{\pi}\bar{G}\frac{\partial\theta}{\partial\psi} - PrH\frac{\partial\theta}{\partial\eta} = 0. \tag{5}$$

The boundary conditions become

$$\frac{\partial}{\partial\rho}\theta(0, \psi, \eta) = 0, \tag{6a}$$

$$\theta(\infty, \psi, \eta) = 0, \tag{6b}$$

$$\theta(\rho, \psi, \eta) = \theta(\rho, \{\psi + 1\}, \eta), \tag{7a}$$

$$\frac{\partial}{\partial\psi}\theta(0, \psi, \eta) = 0, \tag{7b}$$

$$\left.\begin{aligned} \frac{\partial}{\partial\eta}\theta(\rho, \psi, 0) &= 0 \quad \text{for } \psi < \psi_{st} \text{ and } \psi > \psi_{sl} \\ &= 0 \quad \text{for all } \psi \text{ when } \rho > \rho_s, \end{aligned}\right\} \tag{8a}$$

$$\frac{\partial}{\partial\eta}\theta(\{0, \rho_s\}, \{\psi_{st}, \psi_{sl}\}, 0) \text{ specified} \tag{8a'}$$

or

$$\theta(\{0, \rho_s\}, \{\psi_{st}, \psi_{sl}\}, 0) \text{ specified,} \tag{8a''}$$

$$\theta(\rho, \psi, \infty) = 0. \tag{8b}$$

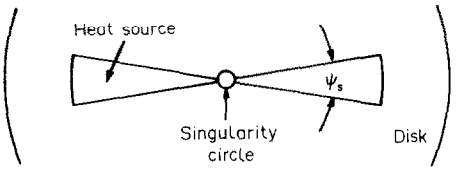

FIG. 2. Singularity circle.

NUMERICAL FORMULATION

The convective diffusion equation for $\theta(\rho, \psi, \eta)$, equation (5), is elliptic. Solution of the corresponding finite difference formulation is achieved by numerical relaxation techniques. In the axial direction both first and second derivatives are approximated by central difference formulae. However, in both the radial and tangential directions central differences are used for the second derivatives while first derivatives are replaced by backward difference expressions to accommodate the strongly convective nature of the flow in these two directions. This technique, which stresses the upstream effects, insures the stability of the solution of the difference equation's matrix, especially at high Re, i.e. large ρ_s. The instabilities which would arise if a central difference formula was used for the radial and tangential convective terms are discussed by Runchal and Wolfstein [15] and by Runchal [16].

The domain of the temperature field is defined for $0 \leqslant \rho \leqslant \rho_{,}$ in the radial direction, $0 \leqslant \psi \leqslant (1 - \Delta\psi)$ in the tangential direction; $\Delta\psi$ being the angle between $\psi = 1$ and the preceding grid point in the tangential direction, and $0 \leqslant \eta \leqslant \eta_{,}$ in the axial direction. A small concentric isothermal region is incorporated in the domain of the numerical solution as shown in Fig. 2. This 'singularity circle' acts to diffuse the influence of the singularity at the disk center as well as to establish a suitable way for satisfying the symmetry condition near the disk center for all ψ's and at all η's. A satisfactory value for $\rho_{,}$ is found by trial to be $15\,\rho_s$ in all cases, and the value of $\eta_{,}$ is dependent on Pr only and can be determined by trial solutions or from ref. [7]. Non-uniform grid spacing is used along each of the three directions ρ, ψ and η. The grid points along the radial and tangential directions are strategically located in high temperature gradient regions, i.e. near the source edges. These locations are continuously updated to minimize errors in the calculations of derivatives. It is fortunate in this problem that at high Re, which corresponds to a large source radius, the errors are largest in the second derivatives, i.e. in the conduction terms which are insignificant in that case. Also, at small Re, the errors are largest in the first derivatives, i.e. in the convection terms which are small in this Re range. This behavior tends to improve the overall accuracy of the results.

The details of the numerical work and error estimates are in [17] and will not be discussed here.

DISCUSSION OF RESULTS

The local heat transfer coefficient h and the local Nusselt number Nu are obtained from the following equations:

$$h(\nu/\omega)^{1/2}/k = \left[\frac{\partial}{\partial\eta}\theta(\rho, \psi, 0)\right] \Big/ \theta(\rho, \psi, 0) \qquad (9)$$

and

$$\begin{aligned} Nu &= h\,r/k, \\ &= h(\nu/\omega)^{1/2}\, Re^{1/2}/k. \end{aligned} \qquad (10)$$

These properties, which are in general dependent on ρ and ψ, are, hereafter, given as ψ-averaged quantities over a source arc area representing the region of influence of the grid points. The average Nusselt number is denoted by

$$\overline{Nu} = \bar{h}r/k.$$

The reliability of the program is checked by initially running the isothermal disk case. This is achieved by prescribing a constant temperature source with $\psi_s = 1$. The relation $Nu = C\,Re^{0.5}$ is found to be valid, with C equal to $h(\nu/\omega)^{1/2}/k$. For a particular Pr, C depends only on h which is constant everywhere on the isothermal disk surface.

Contrary to the isothermal disk configuration, where conduction effects do not exist, in the case of a power law radial temperature profile, $\theta = B\rho^m$, radial conduction becomes significant at low Re and/or large m. Table 1 compares $h(\nu/\omega)^{1/2}/k$ as given by Hartnett [8], who neglected radial conduction, with the present calculations. The agreement is very good for $m < 2$.

For the sector shaped heat source, sketched in Fig. 1, the results exhibit a substantially different behavior than in the above test cases. A qualitative description of this behavior may be explained as follows. At high Re, where both radial and tangential conduction effects may be safely ignored, equation (5) can be written as

$$Re\frac{\partial^2\theta}{\partial\eta^2} = RePrF\rho'\frac{\partial\theta}{\partial\rho'} + RePrH\frac{\partial\theta}{\partial\eta} + \frac{RePr}{\pi}\bar{G}\frac{\partial\theta}{\partial\psi} \qquad (11)$$

where ρ' is a new variable defined as $\rho' = r/r_s$. Since each term contains the Reynolds number and if one assumes that δ_{th} does not vary with ρ', then $\theta(\rho, \psi, \eta)$ and its derivatives are independent of Re. When the disk is isothermal, the third term on the RHS of equation (11) becomes identically zero and solution of

Table 1. Data comparison for an isothermal disk and a power law temperature distribution, $\theta = B\rho^m$, at $Pr = 0.72$.

$\frac{h(\nu/\omega)^{1/2}}{k}$	m		
	0	1	2
Present work	0.341	0.436	0.519
Hartnett [8]	0.330	0.437	0.524

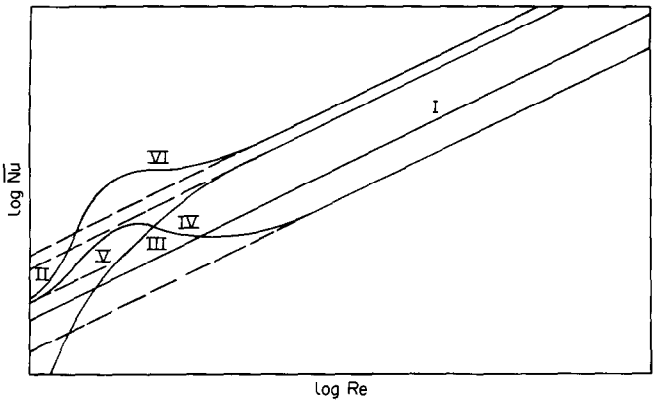

FIG. 3. Qualitative behavior of the various heat transfer mechanisms.

the equation shows that $\bar{h}(\nu/\omega)^{1/2}/k$ is constant. Therefore, $\overline{Nu} = C_I Re^{0.5}$, as given by Curve I in Fig. 3. For a sector shaped source the tangential convection term will only change the solution of this linear equation inasmuch as to show a dependence of $h(\nu/\omega)^{1/2}/k$ on ψ where $\psi_{sl} \leqslant \psi \leqslant \psi_{st}$. Consequently, if $\bar{h}(\nu/\omega)^{1/2}/k$ is ψ-averaged, $Nu = C_{II} Re^{0.5}$ will be expected, with C_{II} dependent on the source geometry and always greater than C_I as given by Curve II in Fig. 3. As the Re decreases, the assumption that δ_{th} is constant becomes invalid. Millsaps and Pohlhausen [6] showed that δ_{th} increases as the center of the disk is approached. This behavior is also observed in this study as will be seen later. The increase in the thermal boundary layer thickness will reduce the $\overline{Nu}$ and the overall behavior of equation (11) may be described by Curve III in Fig. 3. At very low Re convective terms may be neglected altogether and equation (5) becomes a pure conduction equation as follows:

$$\frac{1}{\rho'}\frac{\partial\theta}{\partial\rho'} + \frac{\partial^2\theta}{\partial\rho'^2} + \frac{1}{\rho'^2\psi_s^2\pi^2}\frac{\partial^2\theta}{\partial\psi'^2} + \psi_s^2\frac{\partial^2\theta}{\partial\eta'^2} = 0 \quad (12)$$

where η' and ψ' are new variables defined as

$$\eta' = z/r_s\psi_s,$$

$$\psi' = \psi/\psi_s = \phi/\phi_s.$$

The fourth term in equation (12) balances the remaining three. At large ρ' the first three terms (order $1/\rho'^2$) as well as the axial conduction term are small. However, the $\overline{Nu}$ must still be proportional to $Re^{0.5}$ in the limit as $\partial^2\theta/\partial\eta'^2 \to 0$ which represents an isothermal disk. At small ρ' and ψ_s, radial and tangential conduction become significant, thus, considerably increasing axial conduction as well as the $\overline{Nu}$. This behavior at large and small ρ' is given by Curve IV. It will be shown in the following paragraphs that Curve IV must merge with Curve V as $\rho' \to 0$. The solution obtained in this work is represented by Curve VI which is the combined effects of Curves III and IV.

The effects of the sector angle ψ_s, at a particular Pr, on the $\overline{Nu}$ behavior are shown in Fig. 4. When the source is at constant temperature, a region near $Re \approx 10$ shows a bulge in the $\overline{Nu}$ vs Re distribution. This

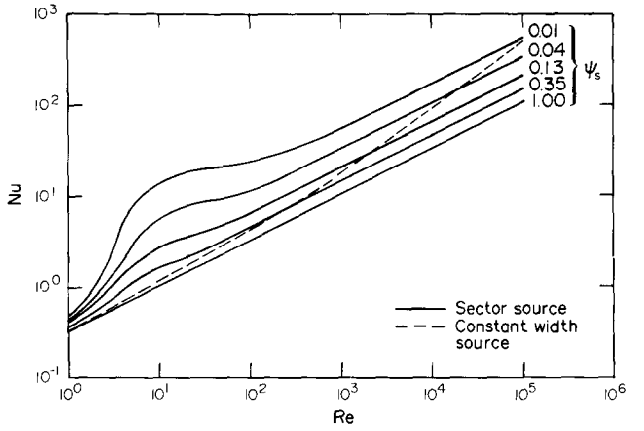

FIG. 4. Influence of source width on $\overline{Nu}$ vs Re relation, $Pr = 0.72$.

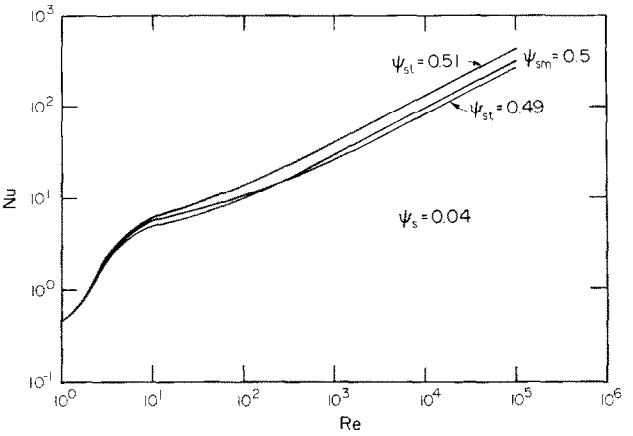

FIG. 5. Local heat transfer at different locations on the heat source.

signifies the increased axial conduction effects over those observable at large Re as previously discussed. The amplitude of the bulge above the line given by $\overline{Nu} = C\,Re^{0.5}$ decreases with increasing sector angle ψ_s. However, this bulge may vanish altogether if the radius of the 'singularity circle', which is at constant temperature, is made large enough. Several check runs indicate that the $\overline{Nu}$ vs Re relation at higher Re is not affected by the size of this circle. The relation $\overline{Nu} = C_V Re^{0.5}$ is valid in the region $0 < Re < 1$ where C_V is always greater than C_I and C_{IV} due to the finite nature of the isothermal region which results in finite radial conduction effects at its boundary.

Due to the tangential asymmetry of the temperature field at high Re the local Nu at the leading edge of the source (the edge that first meets the oncoming fluid stream) is higher than that at the trailing edge. The Nu at the source mid-point is somewhere in between but closer to the source trailing edge. At low Re and due to the nearly symmetric temperature profile in the conduction dominated region, the Nu at the source mid-point is lower than its values at both edges as shown in Fig. 5. This behavior can also be ascertained from the tangential temperature profiles given in Figs. 7 and 8. It should be noted here that at large Re the local Nu is linear with $Re^{0.5}$. Therefore, the averaging process used to present the data of Fig. 4 does not affect the qualitative behavior of the solution.

Figures 6–9 show typical temperature profiles along the radial, tangential and axial directions for a constant temperature heat source. In Fig. 6 the radial temperature distribution is self-explanatory except near the disk center and at small axial distances. Strong tangential conduction creates a relatively cool region which vanishes at higher elevations when, due to flattened temperature profiles, tangential conduction becomes insignificant compared with the dominant radial conduction. At these higher elevations, the profiles monotonically decrease with ρ.

Tangential temperature profiles in the angle range $0 \leqslant \psi \leqslant 1$ are shown in Figs. 7 and 8. At high Re, as in Fig. 7, the temperature profiles are asymmetric as expected in a highly convective field. Furthermore, the maximum temperature occurs near the trailing edge of

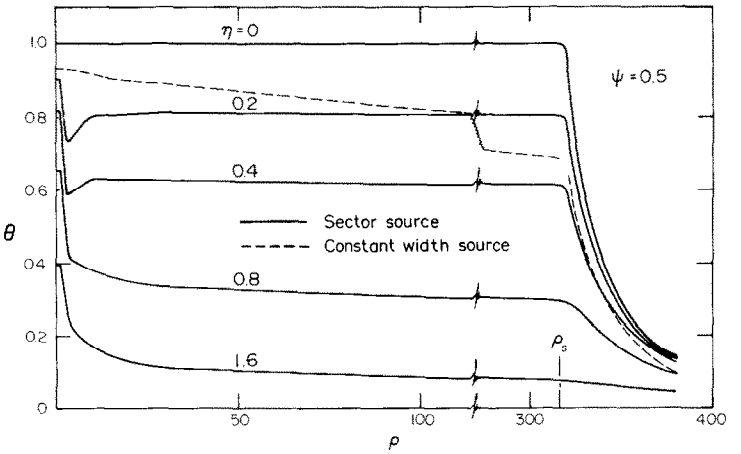

FIG. 6. Radial temperature profiles for $\psi_s = 0.04$, $\eta_s = 8.0$, $Pr = 0.72$.

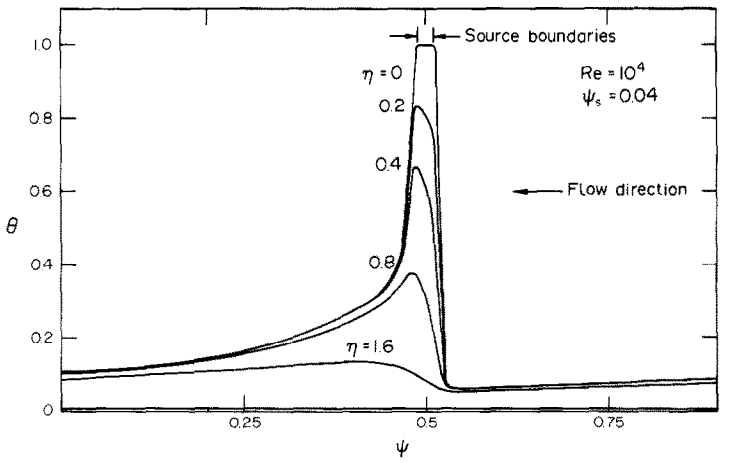

FIG. 7. Tangential temperature profiles at high Re, $\psi_s = 0.04$, $\eta_\infty = 8.0$, $Pr = 0.72$.

the heat source and goes beyond it at higher elevations. On the other hand, at low Re, Fig. 8 shows almost symmetric temperature distribution over the heat source, but the maximum temperature location still shifts towards the downstream side of the source, especially at higher elevations. Figure 9 gives axial temperature profiles over the source, $\psi = 0.5$, and over the adiabatic surface at $\psi = 0.25$, 0.4, 0.47 and 0.6.

Due to the quasi-steady nature of the problem, the thermal boundary layer is found to be axisymmetric. It is interesting to observe that the thermal boundary layer thickness, δ_{th}, defined as

$$\delta_{th} = \eta_{\theta=0.01}(\nu/\omega)^{1/2}$$

decays with radius and the rate of decay increases with decreasing source sector angle ψ_s. This behavior is shown in Fig. 10 and is attributed to the requirement of tangential heating from a finite size source.

Heat transfer from a heated constant width source passing through the disk center can be inferred from sector source data due to the linearity of the problem. For a given source width, local values of Nu are deducible from the present calculations by determining the values of ψ associated with different radial locations along the constant width source. We note here that only near the disk center does the Nu vs Re relation approach the isothermal disk case since ψ becomes very large. In Figs. 4–12 the broken lines represent the heat transfer characteristics of a constant width diametrical heat source. The relation $\overline{Nu} = C\,Re^{0.5}$ is not generally valid in this non-axisymmetric case where the source area does not vary with radial distance as in the cases of an isothermal disk, a disk with a ring source [14], or a sector-shaped source. Another important difference is the disappearance of the conduction bulge near the disk center due to the large values of ψ_s in that region.

Data at different Pr (not shown here) indicates that increased Pr produces an increase in C. A similar effect is produced when ψ_s is reduced. Two small values of ψ_s, 0.005 and 0.00006 are calculated with a considerably increased number of grid points. The rate of con-

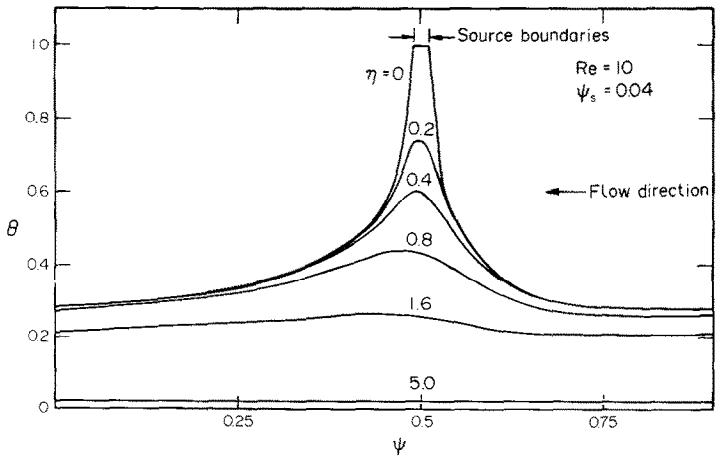

FIG. 8. Tangential temperature profiles at low Re, $\psi_s = 0.04$, $\eta_\infty = 8.0$, $Pr = 0.72$.

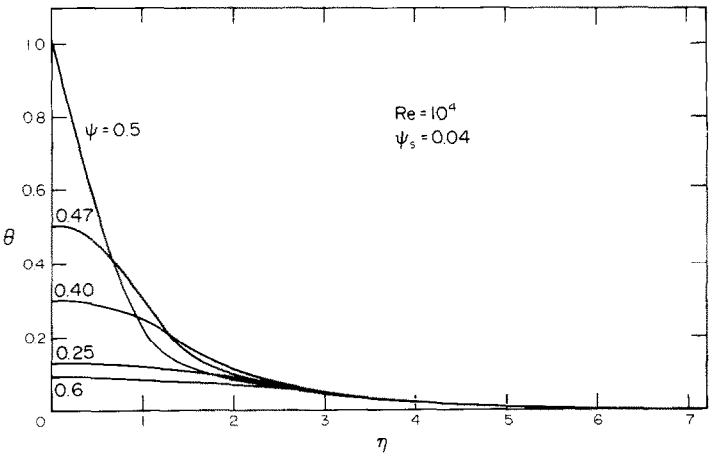

FIG. 9. Axial temperature profiles at high Re, $\eta_\infty = 8.0$, $Pr = 0.72$.

vergence of these runs is very slow and the computation time is excessive. Aside from data for the small ψ_s configuration, they also provided a good check on the quantitative and qualitative results of the original program.

An interesting consequence of the present numerical solution is the relationship between the heat flux per unit area, q, and the local wall shear stress $\tau_{w\phi}$. The dimensionless axial temperature gradient at the wall, Q, is defined as

$$Q = \left.\frac{\partial\theta}{\partial\eta}\right|_{\eta=0} \tag{13}$$

Therefore

$$q = Q\,k(\rho/r)\Delta T \tag{14}$$

where $\Delta T = (T_0 - T_\infty)$ and $\rho/r = (\omega/\nu)^{1/2}$. Figure 11 shows the variation of Q with the tangential friction factor, f_ϕ, over the entire source radial length. This friction factor is defined in [1] as follows:

$$f_\phi = \frac{\tau_{w\phi}}{\frac{1}{2}\mathrm{d}\omega^2 r^2} \tag{15}$$

where

$$\tau_{w\phi} = 0.616\,\mathrm{d}\,\nu^{1/2}\omega^{3/2}r,$$
$$= 0.616\frac{d\nu^2}{r^2}\rho^3. \tag{16}$$

Q, which may be considered as a dimensionless heat flux, attains a constant value after a large peak near the center of the disk which is analogous to the bulge appearing in the $\overline{Nu}$ vs Re figures. A special feature of the relationship between q and $\tau_{w\phi}$ can be seen if we consider the heat transfer from the source at a particular radius on the spinning disk surface. In this case $\tau_{w\phi}$ and q become proportional to ρ^3 and ρ

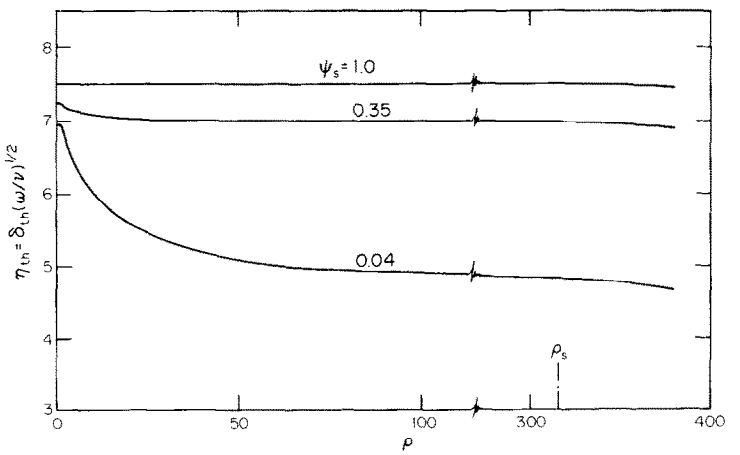

FIG. 10. Thermal boundary layer thickness, $\eta_\infty = 8.0$, $Pr = 0.72$.

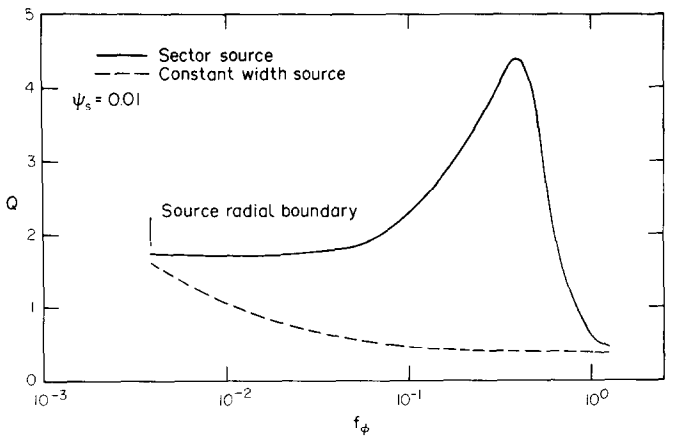

FIG. 11. Correlation between heat flux and friction factor, $Pr = 0.72$.

according to equations (16) and (14), respectively. Therefore, the following relationship is valid:

$$q = A\tau_{w\phi}^{1/3}. \tag{17}$$

Figure 12 shows the behavior of the dimensionless heat flux per unit area q' as a function of the dimensionless tangential component of the wall shear stress $\tau'_{w\phi}$. It is interesting to note that while the heat transfer from the source before and after the bulge is always proportional to $\tau'^{1/3}_{w\phi}$, the mechanisms involved are different and so are the constants of proportionality. At high values of $\tau'_{w\phi}$, the mechanism is convection, while at low values it is mostly conduction. In practice, an additional constant, D, is necessary to model the q vs $\tau^{1/3}_{w\phi}$ behavior. This constant is needed, partially, because of the contribution of natural convection heat transfer while the disk is at rest. This additional constant is usually obtained by calibration.

CONCLUSIONS

The heat transfer coefficient from a sector shaped heat source is shown to be considerably higher than that obtained for an isothermal disk, but approaches it as the source sector angle ϕ_s increases. The relation $\overline{Nu} = C\,Re^{1/2}$ is generally valid even at very low Re, with C varying for different ψ_s, Pr and depending on whether the mechanism is convection or conduction dominated. In a region where both conduction and convection are significant; the region where the bulge appears, C becomes a complex function of Re. The thermal boundary layer thickness is shown to decrease along the radial direction due to tangential heating. Results for a constant width diametrical source may be constructed from those of the sector shaped source. The $\overline{Nu}$ vs Re relation is not linear in this case and the heat transfer increases at a faster rate with increasing Re, especially in the convection dominated region. The 1/3 power law relating the heat flux per unit area to the local wall shear stress is derived from the present calculations.

REFERENCES

1. Th. von Kármán, Über Laminar und Turbulent Reibung, *Z. Angew. Math. Mech.* **1**, 233–252 (1921).
2. W. G. Cochran, The flow due to a rotating disk, *Proc. Cambr. Phil. Soc.* **30**, 365–375 (1934).

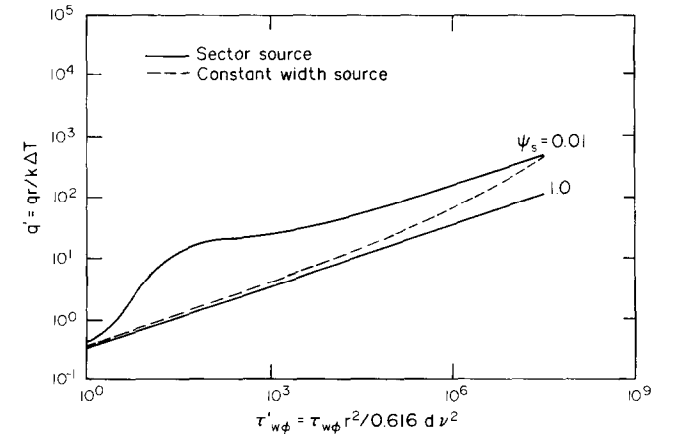

FIG. 12. Correlation between dimensionless heat flux and dimensionless tangential wall shear stress at a given radius.

3. T. S. Cham and M. R. Head, Turbulent boundary layer flow on a rotating disc, *J. Fluid Mech.* **37,** 129–147 (1969).
4. F. F. Erian and Y. H. Tong, Turbulent flow due to a rotating disc, *Phys. Fluids* **14,** 2588–2591 (1971).
5. C. Wagner, Heat transfer from a rotating disk to ambient air, *J. Appl. Phys.* **19,** 837–839 (1948).
6. K. Millsaps and K. Pohlhausen, Heat transfer by laminar flow from a rotating plate, *J. Aeronautical Sci.* **19,** 120–126 (1952).
7. E. M. Sparrow and J. L. Gregg, Heat transfer from a rotating disc to fluids of any Prandtl number, *J. Heat Transfer* **81,** 249–251 (1959).
8. J. P. Hartnett, Heat transfer from a nonisothermal disk rotating in still air, *J. Appl. Mech.* **26,** 672–673 (1959).
9. D. R. Davies, Heat transfer by laminar flow from a rotating disk at large Prandtl numbers, *Q. J. Mech. Appl. Math.* **12,** 14–21 (1959).
10. D. R. Jeng, K. J. DeWitt and M. H. Lee, Forced convection over rotating bodies with non-uniform surface temperature, *Int. J. Heat Mass Transfer* **22,** 89–98 (1979).
11. B. T. Chao and R. Grief, Laminar forced convection over rotating bodies, *J. Heat Transfer* **96,** 463–466 (1974).
12. F. Kreith, J. H. Taylor and J. P. Chong, Heat and mass transfer from a rotating disk, *J. Heat Transfer* **81,** 95–105 (1959).
13. Cz. O. Popiel and L. Boguslawski, Local heat transfer coefficients on the rotating disc in still air, *Int. J. Heat Mass Transfer* **18,** 167–170 (1975).
14. D. L. Oehlbeck and F. F. Erian, Heat transfer from axisymmetric sources at the surface of a rotating disk, *Int. J. Heat Mass Transfer* **22,** 601–610 (1979).
15. A. Runchal and M. Wolfshtein, Numerical integration procedure for the steady state Navier–Stokes equations, *J. Mech. Engng Sci.* **11,** 445–453 (1969).
16. A. Runchal, Convergence and accuracy of three finite differences schemes for a two-dimensional conduction and convection problem, *Int. J. Numer. Methods Engng* **4,** 541–550 (1972).
17. S. E. Tadros, Generalized laminar heat transfer from the surface of a rotating disk, M.Sc. thesis, Clarkson College of Technology, Potsdam, New York (1978).

TRANSFERT THERMIQUE LAMINAIRE GENERALISE A LA SURFACE D'UN DISQUE TOURNANT

Résumé—On résoud numériquement l'équation d'énergie pour un écoulement laminaire incompressible induit par un disque tournant, pour un champ de température tridimensionnel, créé par une source diamétrale, en forme de secteur, logée à la surface du disque dont le reste est adiabatique. Le chauffage est supposé suffisamment doux pour ne pas perturber le champ des vitesses. En conséquence, les effets de la convection naturelle aussi bien que la dissipation visqueuse sont négligés. La technique de surrelaxation simple est appliquée pour obtenir les solutions pour n'importe quelle distribution radiale ou tangentielle de température ou de flux surfacique. On présente plusieurs conditions aux limites dont deux pour lesquelles il existe des solutions exactes. Les résultats obtenus pour différents nombres de Prandtl, et différents angles de source montrent l'existence d'une région à conduction dominante pour les faibles nombres de Reynolds et une région à transport dominant aux grands nombres de Reynolds. On trouve une formule reliant le flux surfacique local à la contrainte tangentielle à la paroi.

ALLGEMEINE BEHANDLUNG DES LAMINAREN WÄRMEÜBERGANGS AN DER OBERFLÄCHE EINER ROTIERENDEN SCHEIBE

Zusammenfassung—Es wird die Energiegleichung für die laminare inkompressible Strömung an einer größen, rotierenden Scheibe numerisch für das dreidimensionale Temperaturfeld gelöst, welches von einer diametrischen, sektorförmigen Wärmequelle erzeugt wird, die sich an der Oberfläche der sonst adiabaten Scheibe befindet. Es wird angenommen, daß die Heizung so schwach ist, daß das Geschwindigkeitsfeld nicht gestört wird. Infolgedessen werden auch die Auswirkungen der freien Konvektion und der zähigkeitsbedingten Dissipationswärme vernachlässigt. Die Anwendungen einfacher Überrelaxationsmethoden genügen, um Lösungen für jede angenommene Verteilung der Oberflächentemperatur oder der Wärmestromdichte in radialer und/oder tangentialer Richtung zu erhalten. Verschiedene Randbedingungen werden erörtert, insbesondere zwei, bei denen unabhängige exakte Lösungen existieren. Die Ergebnisse für verschiedene Prandtl-Zahlen und Winkel der Wärmequelle zeigen, daß bei niedrigen Reynolds-Zahlen eine Zone existiert, in der Wärmeleitung vorherrscht, wogegen bei großen Reynolds-Zahlen eine Zone mit vorherrschender Konvektion auftritt. Zusätzlich wird eine Beziehung zwischen dem lokalen Wärmestrom an der Oberfläche und den Tangentialschubspannungen an der Wand angegeben.

ОБОБЩЕННЫЙ ЛАМИНАРНЫЙ ТЕПЛОПЕРЕНОС ОТ ПОВЕРХНОСТИ ВРАЩАЮЩЕГОСЯ ДИСКА

Аннотация—Дано численное решение уравнения энергии для ламинарного несжимаемого потока жидкости, индуцированного большим вращающимся диском, для трехмерного поля температур, создаваемого диаметральным секторообразным источником тепла, расположенным на поверхности диска, вся оставшаяся часть которой является адиабатической. Предполагается, что мощность источника очень небольшая, так что возмущения поля скоростей не происходит. Следовательно, пренебрегается эффектами естественной конвекции и нагревом за счет вязкой диссипации. Для получения решений при любых заданных радиальных и/или тангенциальных распределений температуры поверхности или теплового потока может использоваться простая методика верхней релаксации. Рассмотрено несколько граничных условий, в том числе два условия, для которых существуют независимые точные решения. Результаты, полученные при различных значениях числа Прандтля и углов сектора, показывают, что при малых значениях числа Рейнольдса можно выделить область с доминирующей теплопроводностью, а при высоких значениях числа Рейнольдса – область с доминирующей конвекцией. Также установлена зависимость между локальным тепловым потоком на поверхности и тангенциальным напряжением сдвига на стенке.